OPTO-ELECTRONICS REVIEW **8**(4), 339–345 (2000)

Silicon thin film multijunction solar cells

A. KOŁODZIEJ[1*], C.R. WRONSKI[2], P. KREWNIAK[1], and S. NOWAK[1]

[1]Department of Electronics, University of Mining and Metallurgy, 30 Mickiewicza Av., 30-059 Kraków, Poland
[2]Centre for Thin Films Devices, The Pennsylvania State University, Pensylvania 16801, USA

The multijunction structure properties of the thin film silicon solar cells and the newest achievements are described. The operation, principle of the solar cell, is based on an effective absorption of incident light and a sufficiently long lifetime of photoexcited electrons and holes such that they can become spatially separated. There are compared different technological methods of obtaining the a-Si:H solar cells leading to their optimal optoelectronic properties. It is also shown some ideas on cells manufacturing partially based on special magnetron sputtering process.

Keywords: tandem solar cell, triple junction solar cell, multijunction silicon solar cell.

1. Introduction

The purpose of this paper is to briefly outline properties of the thin film multijunction silicon solar cells, currently manufactured throughout the world, as well as our experiences in the area. Amorphous silicon solar cells have been fabricated on the different devices structure. These include single junction p–i–n and n–i–p devices as well as Schottky barrier cells, MIS cells and several different types of multijunction cells. Moreover, a-Si solar cells have been fabricated on a variety of different substrates such as glass, metal foils and plastics [1–3]. The major constraint on the substrate material is that it must be able to accommodate temperatures of at least 120°C and not contaminate the a-Si films during deposition [1,2,4,5]. The cell made by Guha with 15.2% efficiency in 1998 is the best checked triple junction solar cell at present. Increase in absorption of incident light, sufficiently long lifetime of photoexcited electrons and holes, and effective separation is the way to obtain better efficiency of a solar cell. As well limitation of light induced degradation which exhibit all amorphous silicon based solar cells is typically 20% to 30% before reaching the steady state. The degradation depends on the device and film structure and deposition condition. At the same time it is important the annealing kinetics of these cells under a variety of illumination and bias condition [3,6,7].

2. A view of solar cell structures

The best commercial tandem solar cell is shown in Fig. 1, Tables 1 and 2 [1,8]. The best triple-junction cells initial 15.2%/stabilised 13.0% have been fabricated on stainless steel foil substrates that were coated with layers of textured silver and zinc oxide (Fig. 2.) In commercial product, the

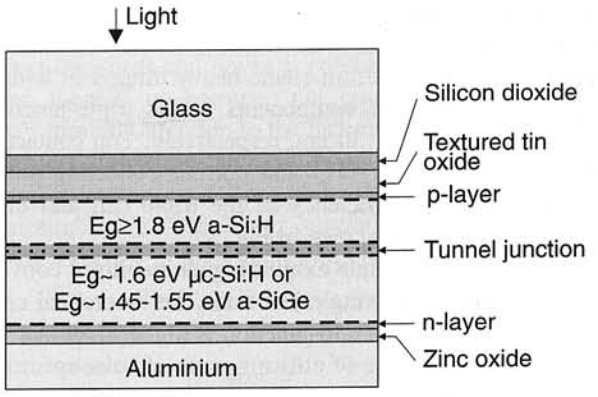

Fig. 1. A schematic of a tandem device structure fabricated on a glass substrate. The commercial structure is made by BP Solarex with efficiency 10.2%.

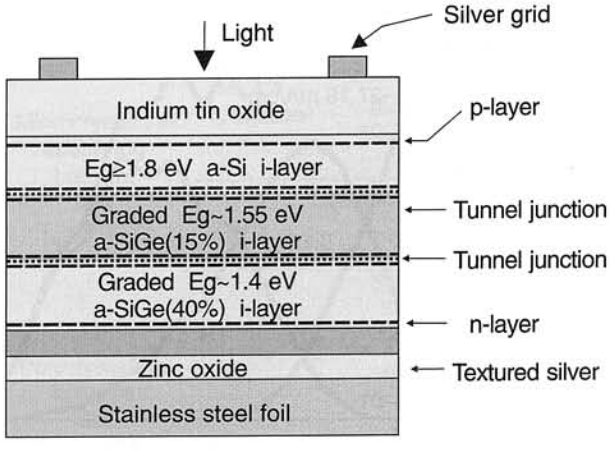

Fig. 2. A schematic of a triple-junction device structure fabricated on a stainless steel substrate. The best triple junction cells initial 15.2% stabilised 13.0% made by Guha in 1998.

*e-mail: kolodzie@uci.agh.edu.pl

Table 1. Amorphous silicon device structures and performance (i* represents an a-SiGe i-layer).

Device structure	Conversion efficiencies (%) (initial/stable)	Organisation
Steel/Ag/ZnO/n-i-p/n-i*-p/n-i*-p/ITO	15.2/13.0	USSC
Steel/Ag/ZnO/n-i-p/n-i*-p/ITO	14.4/12.4	USSC
Glass/SnO_2/p-i-n/p-i-n/ZnO/Ag	12.5/9.0	Fuji Electric
Glass/SnO_2/p-i-n/ZnO/Ag	12.0/8.9	Sanyo
Glass/SnO_2/p-i-n/p-i*-n/ZnO/Ag	11.6/10.0	BP Solarex

back reflector consists of sputtered layers of aluminium and zinc oxide. An a-Si:H n-layer (~20 nm thick) is deposited on the zinc oxide, and then an a-SiGe:H i-layer with a graded germanium concentration is deposited on the n-layer. The structure contains two "tunnel" junctions, each consisting of ~10 nm of "p" mc-Si:H and ~10 nm of "n" a-Si:H. The middle junction also consists of an a-SiGe:H i-layer with a graded germanium concentration, adequately to the back Ge films. The front junction contains of undoped a-Si:H layer from silane heavy diluted in hydrogen. The thickness of components in the triple-junction structure is 100, 110, 130 nm, respectively. Top contact is antireflecting layer of ITO and current collecting silver grid. The quantum efficiency of the triple cell and their three components are shown in Fig. 3.

Multi a-Si PV module exhibit higher stabilised conversion efficiencies than single-junction. The theoretical conversion efficiency for multi-junction is higher than that for single-junction because of utilising more of solar spectrum at a higher net output voltage. Theoretical efficiency: single cell – 28%, tandem cell – 36%, triple-junction cell – 42%. The use of thinner layers improves stabilised performance of multi-junction cell. The assumptions are to produce multijunction solar cells on the base of a-Si:H, mc-Si:H, a-SiGe:H. Volume production is considered by Guha [8].

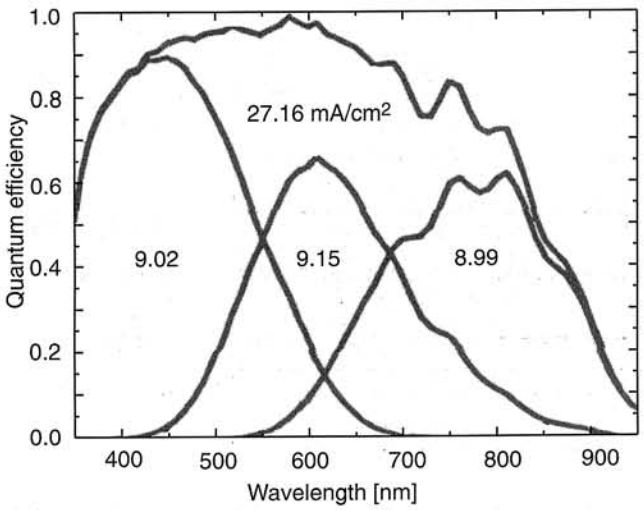

Fig. 3. Quantum efficiency 15.2% of the triple-junction cell made by Guha (1998).

Table 2 summarises commercially available solar cells. The biggest working production line of the thin-layer cells has been depicted in Fig. 4. The Nd-YAG laser is used to scribe through both the Al and a-Si layers to define the individual cell segments. In the case of thin oxide also the Nd-YAG laser with doubled frequency (green) with 15 microns diameter also was used. The series interconnection is completed by using a laser to weld or fuse the Ag ink to the bottom Al contact of the adjacent cell.

3. Manufacturing cost

The projected manufacturing costs are significantly less then 1$/Wp in each case of the thin film solar cells but only

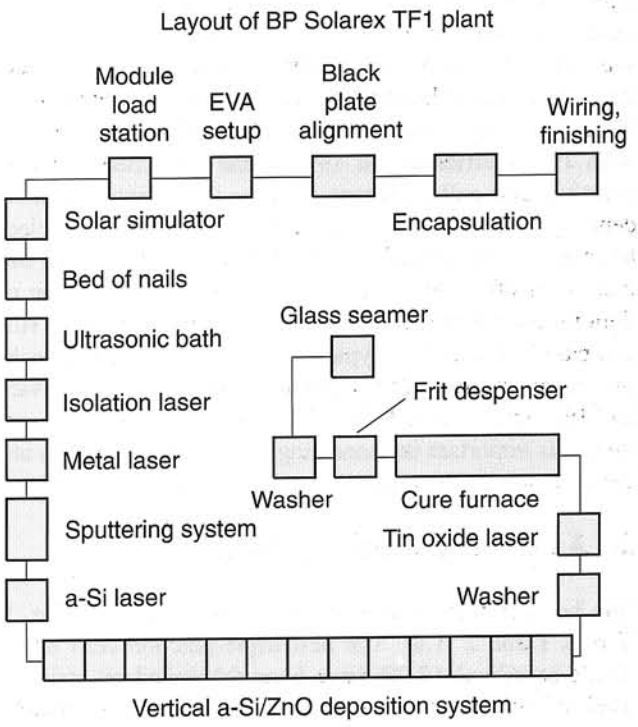

Fig. 4. Schematic of the BP Solarex TF1 plant on Toano, Virginia. After 103 hours to exposure to sunlight 13–17% degradation, 25–30% degradation if contamination.

Table 2. Companies commercialising a-Si PV Technology.

Company	Best stabilised efficiency (%)/(module size)	Module configuration
Kaneka	8.1%/(0.414 m^2)	Single-junction on glass
Sanyo	9.5%/(0.12 m^2)	Tandem on glass
BP Solarex	8.1%/(0.36 m^2)	Tandem on glass
USSC	10.1/(0.09 m^2)	Triple-junction on steel

for production of capacity of greater than 60 MW_p per year (see Fig. 5). If optimisation of efficiency of the solar energy conversion of a module, in respect of its production costs, is the basic criteria of progress, then not only in the future but also now, solar cells produced by thin film, low temperature, vacuum physical or chemical techniques are competitive to expensive monocrystalline solar cells. The major cost elements for a-Si tandem modules are: framing and encapsulation 37%, tin oxide coated glass substrate and back glass plate ~23%, semiconductor feedstock materials and utilisation with GeH_4 ~13% and with SiH_4 ~2%.

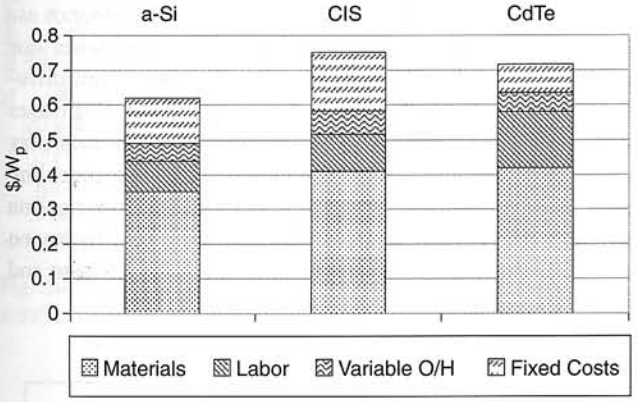

Fig. 5. Projected manufacturing costs for a-Si, CIS and CdTe thin film PV modules made in plants with 60 MW_p/year capacity.

4. Deposition techniques and technology of thin silicon films

To obtain the necessary properties of the produced layers (e.g., desirable chemical bonds) the right temperature and precursor particles must be present. For example, if temperature of the bulk substrate is lowered then the nucleation area of the layer should be energetically activated with other means. The microwave plasma methods and other are currently used (Table 3).

In our case of a magnetron sputtering, the electron heating with unbalanced magnetron is used to the surface activation of the proper precursors in the nucleation area. Thanks to the special system architecture, as well as magnetron source configuration and magnetron-sample configuration, not only bulk temperature can be lower, but also much higher atomisation and ionisation degree of H_2 can be achieved than in the RFCVD method. This, in turn, opens a possibility of achieving layers approaching high incorporation of hydrogen. In that manner it is possible to obtain device quality wide band gap a-Si:H as well as control microcrystalline process stimulated by hydrogen [4,5,9,10]. Considerations on amorphous microcrystalline phase shift were carried out in Refs. 4, 11–13. Figure 6 presents thin silicon layers, aligned in short and long-term orders. They can be obtained by different techniques depending on deposition rate, hydrogen dilution and substrate temperature. The existence of the protocrystalline layers comes from indirect measures and physical continuity philosophy. However, there is no roentgen nor raman evidence of them. Let's turn our attention to the fact that hydrogen stimulated microcrystallisation can lead through voids and big $(SiH_n)_m$ complex to big crystallites and nonuniform layer what is undesirable, or – at lower sputtering rates by scattered point defects – to high nanocrystallisation and those layers

Amorphous various methods T_s = 100–250°C	H_2 dilution	Good quality DOS = 10^{16} cm^{-3}
Protocrystalline RFCVD T_s > 200°C	1 Å/s H_2 dilution	The best quality DOS < 3×10^{15} cm^{-3} short term order 1–2 neighbors
Microcrystalline sputtering hot-wire MW T_s > 200°C	>6 Å/s H_2 dilution	Lower density ρ (g/cm^{-3}) voids $(SiH_n)_m$ complexes 10–50 nm crystallites 20% μc phase
	4–5 Å/s H_2 dilution	Greater density ρ (g/cm^{-3}) long term order 2–3 neighbors 5–10 nm crystallites 50–70% μc phase
Polycrystalline hot-wire MW T_s > 400°C		4% of H in the film 10–100 nm crystallites 90% poly phase

Fig. 6. Low temperature device quality various thin silicon films (DOS – density of states in the gap).

Table 3. Characteristic quantities of various deposition techniques (laboratory systems) for the deposition of device-quality hydrogenated amorphous silicon.

Parameter	PE CVD 13.56 MHz	VHF CVD 60.80 MHz	MW CVD 2.5 GHz	ECR CVD	HW CVD	PBD down-stream	RMS
Electron density n_e (cm^{-3})	10^9	$(5–10)\times10^9$	10^{10}	10^{11}	$0–10^{11}$	10^{11}	$0–10^{10}$
Ionisation ratio	10^{-5}	10^{-4}	10^{-3}	10^{-2}	0	10^{-3}	10^{-3}
Sheath voltage (V)	40–50	5–15	–	0.2	0	2	–
Deposition rate (Å/s)	2	20	20	25	20	100	0–30
Process pressure (mbar)	0.5	0.2	10^{-1}	10^{-3}	10^{-2}	0.2	10^{-2}
Decomposition power consumption (W)	4	4	100	300	240	5000	200
Typical sample size (cm^2)	100	100	100	25	60	25	1000
Typical deposition temperature (°C)	250	200	150	200	350	450	100–200

expose excellent optoelectronical properties. With relatively low hydrogen dilution R = H_2/Si:H_4 of 10–20 the growth of a-Si:H films not only becomes dependent on the substrate but also changes the grows so as to make the microstructure thickness dependent. As a result during grows the materials, which are initially amorphous eventually become microcrystalline (Fig. 7) [7]. Figure 8 depicts changes of the photoconductivity in respect to the hydrogen dilution and bulk temperature changes [14].

5. Light induced degradation

All amorphous silicon based solar cells exhibit varying degrees of light-induced degradation depending on the device structure and deposition conditions (Figs. 9 and 10). Single-junction a-Si:H cells typically degrade about 20–30% before reaching a steady state while a-Si:H/a-SiGe:H tandem cells typically degrade about 10–18%. However, there is still considerable debate about the microscopic origin of the light-induced degradation and whether hydrogen motion plays a role [7,15]. Thus, in every case, the kinetics associated with degradation and annealing are slower for a-SiGe:H cells than for a-Si:H cells. The deuterium diffusion studies indicate that the hydrogen in a-SiGe:H diffuses more slowly than that in a-Si:H, hydrogen motion may play a role in determining both the degradation and annealing kinetics of the devices. Therefore, the current investigation provides support for models which assume that hydrogen motion is associated with the light-induced degradation and annealing of a-Si:H based alloys.

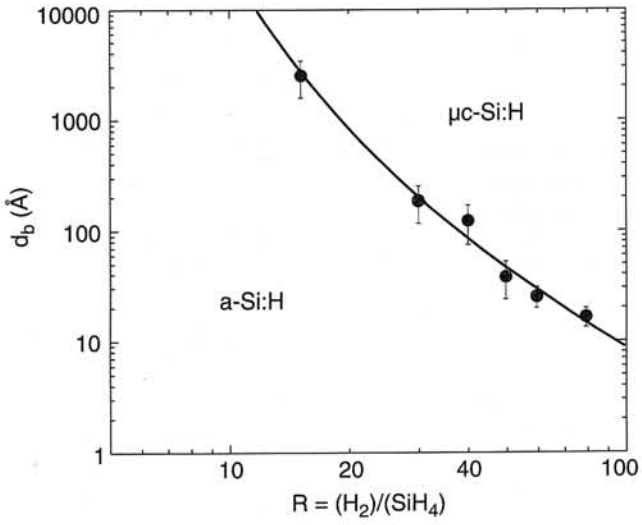

Fig. 7. Film thickness d_b for the phase transition a-Si:H to mc-Si:H plotted versus the hydrogen dilution ratio of silane.

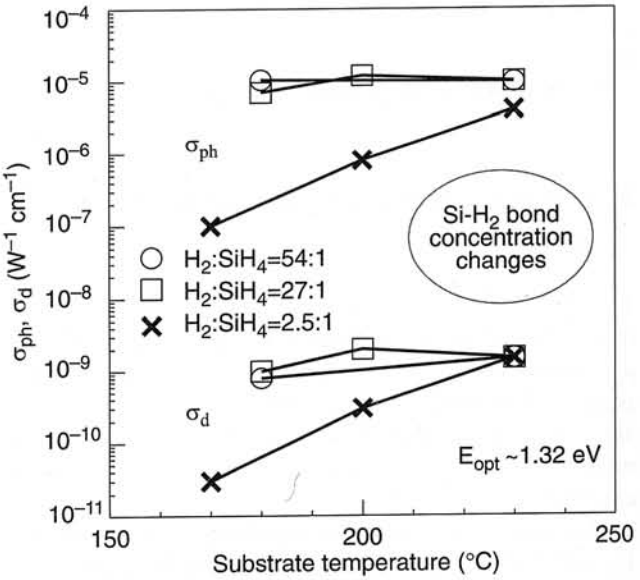

Fig. 8. The relationship between the substrate temperature and photo σ_{ph} and dark σ_d conductivity as a function of hydrogen dilution ratio. The Eopt of all samples is kept constant at 1.320 ±0.005 eV determined from hν vs. $(\alpha h\nu)^{1/3}$ plots (after Ref. 14).

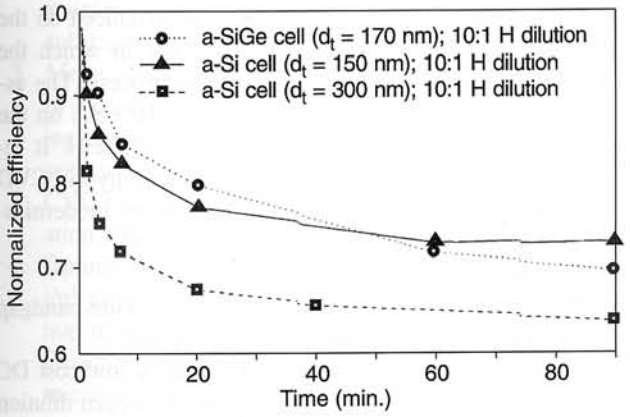

Fig. 9. The normalised conversion efficiency of a-Si:H and a-SiGe:H cells as a function of time exposed to 60 suns illumination at 60°C under open circuit.

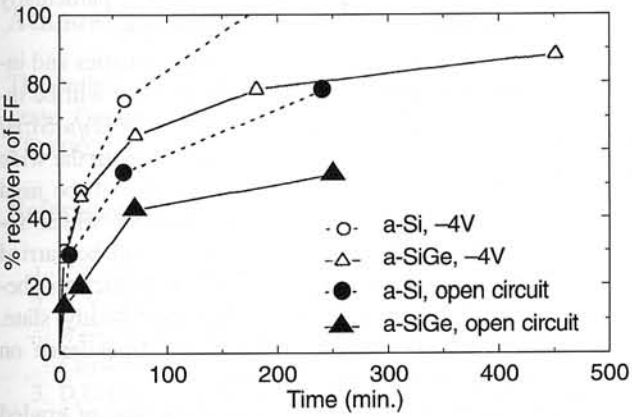

Fig. 10. The recovery of the fill factor of degraded a-Si:H and a-SiGe:H cells as a function of annealing time at 100°C in the dark for different bias conditions.

6. A role of p^+/i, i/p^+, tunnel p/n, tunnel n/p, n^+/i, i/n^+ junctions

The built-in potential in p-i-n a-Si:H, which is determined by the separations of Fermi levels E_{FP} in the p and E_{FN} in n contacts, is in this case 1.3 V. Built-in potentials like this, not only to allow high value of V_{OC} to be obtained, but also result in built-in electric fields greater than 10^4 V/cm across cells with i-layers less than 1 μm thick. The efficient collection of carriers generated by sunlight in the i-layers now no longer depends on purely diffusive processes, but also relies on the electric fields to make the average time taken to transit the i-layers shorter than their recombination lifetimes. Such field-assisted carrier collection, however, is very sensitive to the thickness of the i-layer, L, being approximately proportional to $1/L^2$ rather than 1/L. This makes it difficult to maintain efficient carrier collection when the i-layer is made thicker in order to increase the amount of absorbed sunlight in a cell. The fill factor is the cell parameter which is most sensitive to the cell thickness

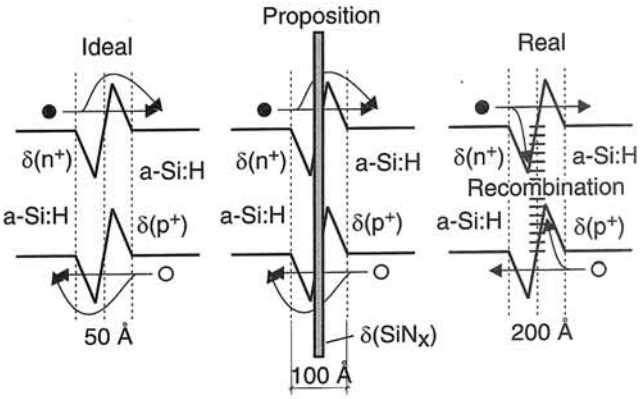

Fig. 11. The role of the tunnel junction $\delta(n^+)$ and $\delta(p^+)$ in the multijunction structure.

as well as the states in the gap since they determine the carrier lifetimes and the space charge densities that are responsible for the electric field distributions across the i-layers.

This n–p junction is often referred to as a tunnel junction but actually functions as a recombination junction in electrically connecting the two p–i–n junctions of the tandem structure in series (Fig. 11). It is not effective (recombination, overlap migration of donors and acceptors). His task is to pull electrons from amorphous range characterised by low electric fields before they recombine. Inherent fields (built-in) are much stronger than outer fields. There are technological experiments stabilising and creating new properties of examined structure. Additional SiN very thin film which play a role of ions (atoms) diffusion blocking barriers and simultaneously tunnel layer. The structures treated by a pure nitrogen plasma flux by a few minutes have also less intersurface recombination centres [5,7]. It is interesting to note that when the cell is illuminated the lowest electric field and the highest recombination rate are positioned close to the i/n interface (Figs. 12 and 13). This result suggests that one has to pay attention not only to the p/i

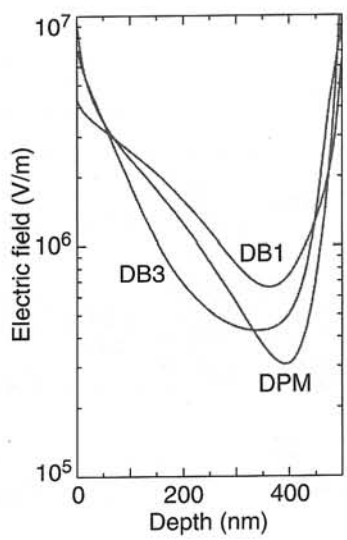

Fig. 12. The electric field profile in the intrinsic layer of an a-Si:H p-i-n solar cell under short circuit current conditions.

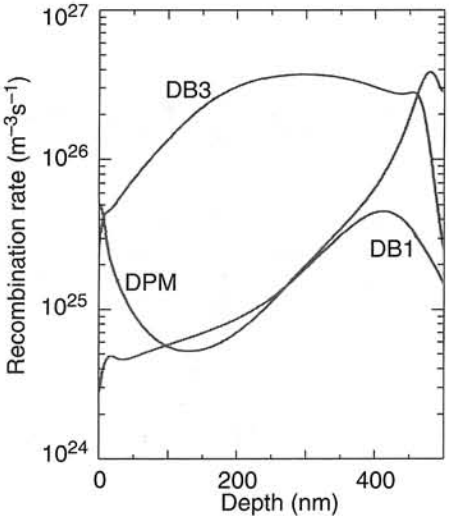

Fig. 13. The recombination rate profile in the intrinsic layer of an a-Si:H p-i-n solar cell under short circuit current conditions.

interface but also to a proper design of the i/n region to improve the collection from this part of the solar cell. Not only an increase in the total density of defect states influences the performance of the cell but also the spatial distribution of the defects plays an important role. This is evident from the comparison of the simulated quantities corresponding to DBI and DPM parameters (DBM – dangling bonds model, DPM – defect pool model). This implies the need of the placing an extra n/p in the n/i region [16–18].

7. Experiments planned to be performed in Krakow

The purpose of this project is the using of wide bandgap a-Si:H for tandem or triple junction cell applications. Two versions of the photovoltaic structures are planned to make (Fig. 14). Worthy of attention is the one produced on the laminated copper or aluminium polyamide in which the metal layer is removed at the end of the process. The assumptions are to produce multijunction solar cells on the base of a-Si:H, μc-Si:H, a-SiGe:H and μc-SiGe:H. It requires also to build a vacuum device based on hybrid CVD technique and reactive magnetron sputtering by modernisation of existing arrangement in our laboratory.

Topics of the work are as follows

1. The possibility of the using of ≥1.8 eV wide bandgap a-Si:H for triple junction cell applications:
   (a) amorphous silicon will be prepared by low cost DC magnetron sputtering under strong hydrogen dilution conditions approaching high incorporation of hydrogen to obtain device quality wide bandgap a-Si:H. Our proposal is to use the special mode of the reactive magnetron sputtering technique to create aforementioned i a-Si:H and n^+a-Si:H layers, particularly in low temperature deposition conditions.
   (b) light and dark current-voltage characteristics and internal quantum efficiency characteristics will be investigated in specular TCO/n^+(a-Si:H)/a-Si:H/Nickel Schottky barrier cell structures with the wide bandgap a-Si:H. These characteristics will be used for analysing a gap state distribution, which includes charged defects. The studies will be carried out on a structure with different i layer thickness between 0.2–0.5 μm after a degraded steady state. There will be presented fill factor dependence on light, field, thickness and time.
2. The comparison between various properties of graded a-SiGe:H layers obtained by CVD and special mode of magnetron sputtering in temperature 250°C and obtained in temperature 100°C will be performed carrying out a number of systematic experiments on TCO/n^+(a-Si:H)/ a-Si:H/Nickel Schottky structures made on

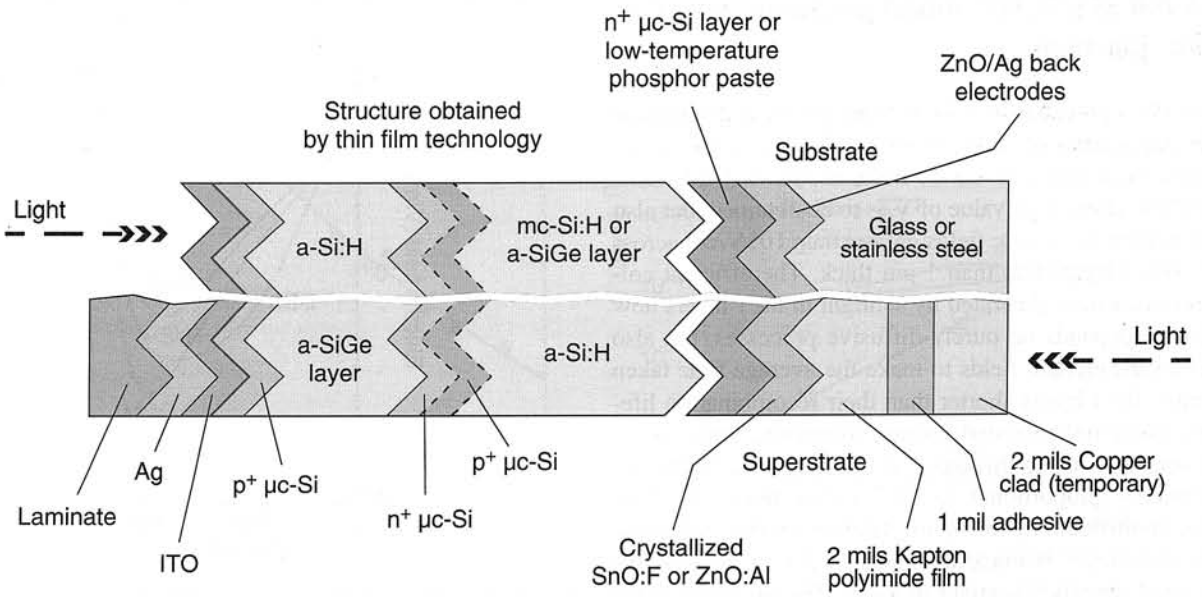

Fig. 14. Two versions of dual or triple junction solar cells.

stainless steel, glass and laminated Al polyimide foil substrates.

3. Modernisation of regular equipment and optimisation of technology based on CVD towards equipment making possible obtaining multijunction solar cell structure with wide band gap a-Si:H and graded a-SiGe:H using CVD technique with increased hydrogen plasma ionisation and using special magnetron mode.
4. Optimisation of p^+/i, i/p^+, tunnel p/n, tunnel n/p, n^+/i, i/n^+ junctions by using low cost DC magnetron sputtering under strong hydrogen dilution conditions approaching high incorporation of hydrogen to obtain microcrystalline Si:H. Our proposal is to use additional intersurface nitridation which is ion diffusion migration resistant during solar cell production.
5. Cost and technology optimisation of the production method of the textured ZnO films.

Acknowledgements

The author acknowledges support for this research under State Committee to Scientific Research Contract no. 8T11B02212.

References

1. C.R. Wronski and D.E. Carlson (private information).
2. J. Yang, A. Banerjee, K. Lord, and S. Guha, *Proc. 2nd World Conf. and Exhibition on Photovoltaic Solar Energy Conversion*, 387–390, Vienna, Austria, 1998.
3. D.E. Carlson, L.F. Chen, G. Ganguly, G. Lin, A.R. Middya, R.S. Crandall, and R. Reedy, *Mat. Res. Soc. Symp. Proc.* **557**, 395–400 (1999).
4. A. Kołodziej, P. Krewniak, and R. Tadeusiewicz, *Mat. Res. Soc. Symp. Proc.* **558**, 243–246 (2000).
5. A. Kołodziej, S. Nowak, and P. Krewniak, *Mat. Res. Soc. Symp. Proc.* **452**, 913–918 (1997).
6. D.L. Staebler and C.R. Wronski, *Appl. Phys. Lett.* **31**, 292 (1976).
7. R.J. Koval, J. Koh, Z. Lu, Y. Lee, L. Jiao, R.W. Collins, and C.R. Wronski, "Kinetics of light induced changes in P-I-N cells with protocrystalline Si:H", *Mat. Res. Soc. Symp. Proc.* **557**, 263 (1999).
8. S. Guha, J. Yang, A. Banerjee, K. Hoffman, and J. Call, *Proc. AIP Conf.* **462**, 88–93 (1988).
9. A. Kołodziej, *J. Non-Cryst. Solids* **185**, 168 (1995).
10. J. D. Cohen, D. Kwon, C.C. Chen, H.C. Jin, E. Hollar, I. Robertson, and J.R. Abelson, "Electronic transistions in mixed phase crystalline/amprphous silicon in the low crystalline fraction regime", *Mat. Res. Soc. Symp. Proc.* **557**, 495 (1999).
11. G. Ganguly and A. Matsuda, *J. Non-Cryst. Solids* **198–200**, 559–562 (1998).
12. Z. Lu, H. Jiao, R. Koval, R.W. Collins, and C.R. Wronski, "Characteristics of different thickness a-Si:H/metal Schottky barrier cell structures – results and analysis", *Mat. Res. Soc. Symp. Proc.* **557**, 785 (1999).
13. S. Guha, J. Yang, D.L. Wiliamson, Y. Lubianiker, J.D. Cohen, and A.H. Mahan, *Appl. Phys. Lett.* **74**, 1860 (1999).
14. M. Shima, M. Isomura, E. Maruyama, S. Okamoto, H. Haku, K. Wakisaka, S. Kiyama, and S. Tsuda, *Mat. Res. Soc. Symp. Proc.* **507**, 145–156 (1998).
15. M. Stutzman, *Mat. Res. Soc. Symp. Proc.* **467**, 37–48 (1997).
16. S. Guha, J. Yang, T. Pawlikiewicz, T. Glatfelter, R. Ross, and S.R. Ovshinsky, *Appl. Phys. Lett.* **54**, 2330–2332 (1988).
17. P. Chaterjee, *J. Appl. Phys.* **76**, 1301 (1994).
18. P. Chaterjee, *J. Appl. Phys.* **79**, 7339 (1996).